Polyadenylate-binding protein–interacting proteins PAIP1 and PAIP2 affect translation termination

Received for publication, November 25, 2018, and in revised form, March 29, 2019 Published, Papers in Press, April 16, 2019, DOI 10.1074/jbc.RA118.006856

Alexandr Ivanov[‡§], Ekaterina Shuvalova[‡], Tatiana Egorova[‡], Alexey Shuvalov[‡], Elizaveta Sokolova[‡], Nikita Bizyaev[‡], Ivan Shatsky[¶], Ilya Terenin[¶‖1], and Elena Alkalaeva[‡2]

From the [‡]Engelhardt Institute of Molecular Biology, Russian Academy of Sciences, Moscow 119991, Russia, the [§]Faculty of Bioengineering and Bioinformatics and the [¶]Belozersky Institute of Physico-Chemical Biology, M. V. Lomonosov Moscow State University, Moscow 119234, Russia, and the [‖]Sechenov First Moscow State Medical University, Institute of Molecular Medicine, Moscow 119146, Russia

Edited by Karin Musier-Forsyth

Polyadenylate-binding protein (PABP) stimulates translation termination via interaction of its C-terminal domain with eukaryotic polypeptide chain release factor, eRF3. Additionally, two other proteins, poly(A)-binding protein-interacting proteins 1 and 2 (PAIP1 and PAIP2), bind the same domain of PABP and regulate its translation-related activity. To study the biochemistry of eRF3 and PAIP1/2 competition for PABP binding, we quantified the effects of PAIPs on translation termination in the presence or absence of PABP. Our results demonstrated that both PAIP1 and PAIP2 prevented translation termination at the premature termination codon, by controlling PABP activity. Moreover, PAIP1 and PAIP2 inhibited the activity of free PABP on translation termination *in vitro*. However, after binding the poly(A) tail, PABP became insensitive to suppression by PAIPs and efficiently activated translation termination in the presence of eRF3a. Additionally, we revealed that PAIP1 binds eRF3 in solution, which stabilizes the post-termination complex. These results indicated that PAIP1 and PAIP2 participate in translation termination and are important regulators of readthrough at the premature termination codon.

PABP[3] a multifunctional protein involved in RNA metabolism is a major mRNA-interacting protein in eukaryotic cells. The N-terminal half of the protein contains four RNA-recognition motifs (RRMs) (Fig. 1*A*), and two of these (RRM1/2) specifically bind 12 adenines on mRNA poly(A) tails, whereas the others (RRM3/4), nonspecifically bind any RNA (1). Each RRM has two surfaces, with one capable of binding RNA and the other capable of interacting with the PABP-associated motif (PAM) 1 region of several proteins. The C-terminal domain of PABP (CTC), which binds the PAM2 motif of specific proteins, is joined with the N-terminal portion of PABP by an unstructured linker (Fig. 1*A*) (2).

In animal cells, PABP is controlled by the PABP-interacting proteins PAIP1 and PAIP2. PAIP1 contains PAM1 and PAM2 motifs, as well as a domain homologous to the middle eIF4G domain (MIF4G) (Fig. 1*A*) (3). PAM1 binds the RRM1/2 motifs of PABP with high affinity, whereas PAM2 binds the CTC domain of PABP with low affinity (4). PAIP2 contains only PAM1 and PAM2 domains and binds PABP exclusively (Fig. 1*A*) (5, 6). Similar to PAIP1, the PAM1 motif of PAIP2 efficiently binds the RRM2/3 of PABP, whereas the PAM2 motif binds the CTC domain of PABP with ~100-fold less affinity (5).

PABP is most known for protecting mRNA from degradation (reviewed in Ref. 7), and PABP regulates translation initiation. It binds the N-terminal region of eukaryotic initiation factor 4G (eIF4G), which mutually potentiates the activities of each protein (8). The interaction enhances both PABP binding to the poly(A) tail of mRNA and eIF4G interaction with the cap-binding initiation factor eIF4E (9, 10). In turn, PABP–eIF4G interaction initiates the formation of a closed-loop mRNA structure involving adjacent 5′ and 3′ ends (11), with this structure significantly enhancing translation efficiency, although details associated with this process remain unclear (12, 13). Interaction of PAIP1 with PABP stimulates translation *in vivo* (3), and PAIP1 also binds several translation–initiation factors, such as eIF4G, eIF4A, and eIF3, to form the ternary complexes PAIP1–PABP–eIF4G, PABP–PAIP1–eIF4A, and PAIP1–eIF3–eIF4G (3, 14). These (or higher order) complexes stabilize the closed-loop mRNA structure and stimulate translation. In contrast with PAIP1, PAIP2 inhibits translation (6), with PABP binding of an mRNA poly(A) tail inducing PABP bending at a point between the RRM2 and RRM3 domains, whereas interaction with PAIP2 unbends PABP and prevents the binding with the poly(A) regions of RNA (15). Moreover, PAIP2 also competes with eIF4G for PABP binding (16). These two properties of PAIP2 appear to determine its translation–suppression capacity.

Another significant PABP activity involves the stimulation of translation termination. Eukaryotic translation termination

This work was supported by Russian Science Foundation Grant 14-14-00487, Russian Foundation for Basic Research Grants 15-04-08174 and 16-04-01628; and Program of Fundamental Research for State Academies Grant 1201363822. The authors declare that they have no conflicts of interest with the contents of this article.

This article contains Figs. S1–S4.

[1] To whom correspondence may be addressed. Tel.: 74959394857; Fax: 74959390338; E-mail: terenin@genebee.msu.ru.

[2] To whom correspondence may be addressed. Tel.: 74991359977; Fax: 74991351405; E-mail: alkalaeva@eimb.ru.

[3] The abbreviations used are: PABP, polyadenylate-binding protein; PAIP, poly(A)-binding protein-interacting protein; preTC, pretermination complex; TC, termination complex; postTC, post-termination complex; eRF, eukaryotic release factor; PTC, premature termination codon; RRM, RNA-recognition motif; PAM, PABP-associated motif; eIF, eukaryotic initiation factor; MIF4G, middle eIF4G domain; nt, nucleotide(s); GST, glutathione *S*-transferase; GDPCP, 5′-guanosyl-methylene-triphosphate.

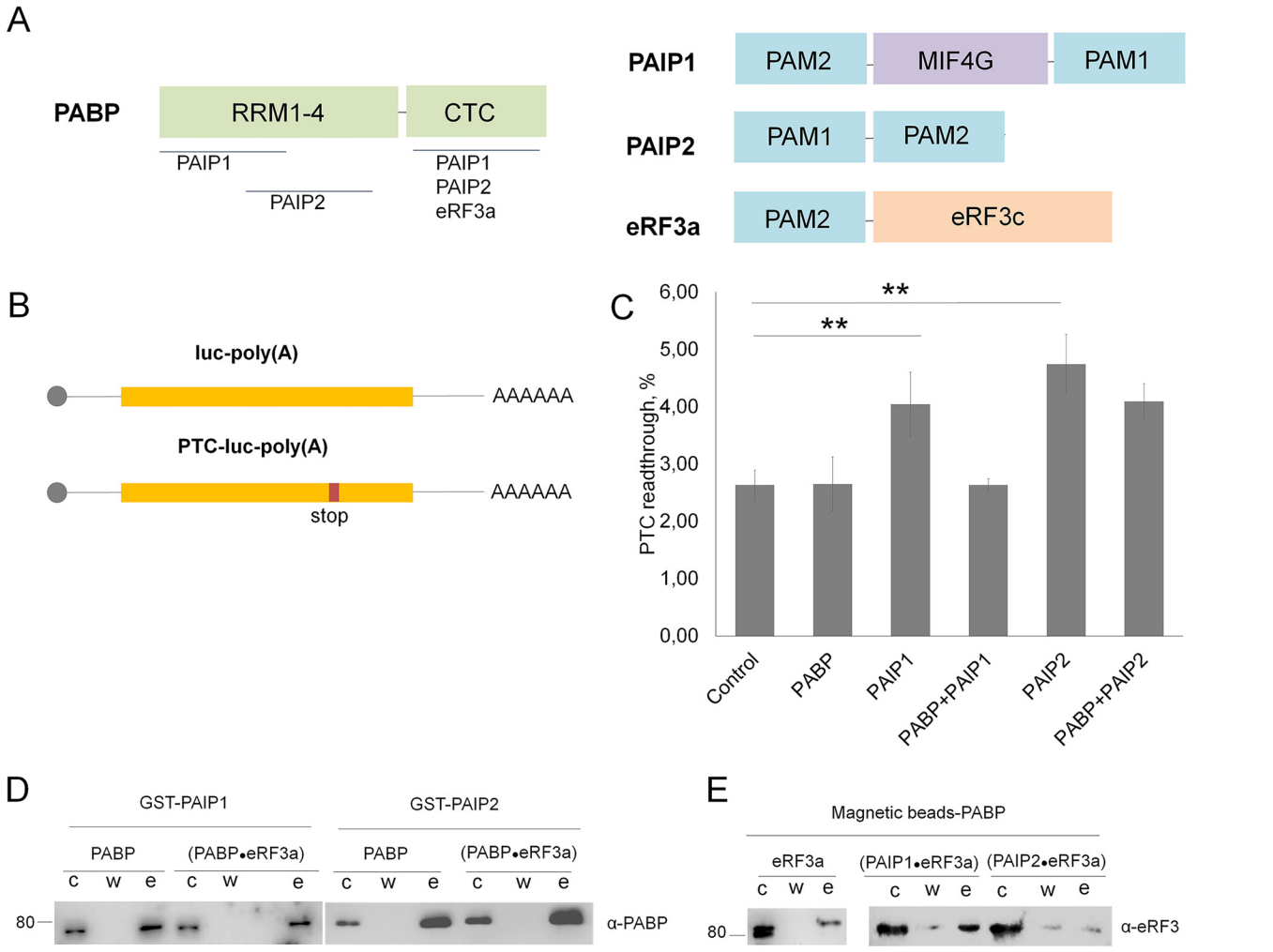

Figure 1. Effect of PAIP1 and PAIP2 on translation termination in the cell-free translation system and interaction of PAIP1 and PAIP2 with PABP and eRF3a. *A*, schematic showing the domain organization of PABP, PAIP1, PAIP2, and eRF3a. Sites of interaction between different PAM motifs with PABP domains are marked with *gray lines*. *B*, schematic showing the organization of model luc–poly(A) and PTC–luc–poly(A) mRNAs. *C*, effect of PAIP1 and PAIP2 on the PTC readthrough of PTC–luc–poly(A) mRNA in Krebs-2 cell lysate. **, $p < 0.01$; *, $p < 0.05$, *t* test. *D* and *E*, interaction of PAIP1 and PAIP2 with PABP and eRF3a according to GST or magnetic bead pulldown assays. *D*, PAIP1 and PAIP2 binding with PABP or the PABP– eRF3a complex according to anti-PABP staining. *E*, PABP binding with eRF3a or PAIP1 + eRF3a, PAIP2 + eRF3a according to anti-eRF3a staining. For detection, antibodies raised against PAPB and eRF3 were used. *c*, control protein; *w*, wash; *e*, elution by protease cleavage of GST-tagged proteins.

requires two release factors: eukaryotic polypeptide chain release factor (eRF) 1 and eRF3 (17, 18). eRF1 is responsible for stop codon recognition and induction of peptidyl-tRNA hydrolysis (19–23). Additionally, eRF1 interacts with eRF3, a GTPase that ensures loading of eRF1 onto the ribosome (17, 20, 24) and induces conformational rearrangement of the latter (25–27). eRF3 is comprised of an N-terminal domain containing the PAM2 motif, which binds PABP, and the core of the protein (eRF3c), which interacts with eRF1 (Fig. 1*A*) (28). PABP binding to eRF3 enhances the loading of the release factors onto the ribosome (29, 30), thereby preventing interaction of an eRF1–eRF3 complex with the nonsense-mediated decay machinery and inhibiting stop codon readthrough (31). Notably, some organisms lacking dedicated stop codons have been proposed to utilize this PABP-related activity to discriminate between sense and stop codons (23, 32–34).

Because PAIP1/2 and eRF3 interact with the same CTC domain of PABP, they can theoretically compete for binding to PABP, thereby affecting the efficiency of translation termination and initiation. To clarify this issue, we analyzed the effect of PAIP1 and PAIP2 on the stop codon readthrough and translation termination efficiency in the presence of PABP. We found that both PAIP1 and PAIP2 increased PTC readthrough in a cell-free translation system. In the reconstructed translation system, PAIP2 abrogated the stimulating effects of free PABP on translation termination, most likely by preventing PABP interaction with eRF3. By contrast, under the same conditions, PAIP1 exhibited a dual effect on translation termination first by competing with eRF3 for binding with free PABP to decrease termination efficiency and second by interacting with eRF3 to increase the efficiency of postTC formation, even in the absence of PABP. Based on our observations, we propose that one of the functions of PAIP1 and PAIP2 during translation is to prevent translation termination at PTCs via sequestration of unbound PABP.

Table 1
Amount of endogenous proteins in 10 μl of Krebs S30 lysate

Protein	Amount
	pmol
PABP	30
PAIP1	0.03
PAIP2	Not detected
eRF1	20
eRF3a	2

Results

PAIP1 and PAIP2 increase PTC readthrough in cell-free translation

To examine how PAIPs modulate the activity of PABP during translation termination, we first tested whether PAIPs influence stop codon readthrough. We constructed a model mRNA containing PTC in the coding sequence of firefly luciferase (Fig. 1*B*). Because PABP affected both translation initiation and termination, we compared the translation rate in the cell-free system of model mRNAs differing only by the presence/absence of PTC in the luciferase coding sequence. PTC readthrough was calculated using the following formula: (translation rate of the PTC-luc mRNA/translation rate of the luc mRNA) × 100, and was expressed in percentages. As a result, we determined PTC readthrough efficiency under various conditions and excluded the effects of added proteins on the other stages of translation (Fig. 1*C*). The cell-free translation was performed in the nuclease untreated S30 extract from ascites cells Krebs-2 (Fig. S1). Amounts of PAIP1, PAIP2, PABP, eRF1, and eRF3a in Krebs-2 extract were determined by Western blotting analysis with specific antibodies (Table 1 and Fig. S2*A*).

The addition of exogenous PABP did not influence readthrough at the PTC–luc—poly(A) mRNA. Because the concentration of endogenous PABP was 20 times higher than the exogenous (Table 1), added PABP was unable to affect readthrough (Fig. 1*C* and Fig. S2*A*). Conversely, the addition of more than 50-fold excess of PAIP1 and PAIP2 to the S30 extract (2 and 0.5 pmol, respectively; Table 1) resulted in a significant increase of readthrough (with increases of 1.5- and 1.8-fold, respectively) as compared with the control (Fig. 1*C*). The addition of 30 pmol of PAIP1 or PAIP2 to the S30 extract resulted in increase of readthrough in the presence of PAIP1 and did not change readthrough in the presence of PAIP2 as compared with experiments with the lower concentrations of exogenous proteins (Fig. S2*B*). Simultaneous addition of PABP and PAIP1 restored PTC readthrough level to the control one. Consequently, exogenous PABP eliminated PAIP1-induced inhibition of translation through binding with PAIP1 in solution. By contrast, the addition of PABP to PAIP2 only partially decreased PTC readthrough induced by PAIP2 (Fig. 1*C*). To test the effect of the poly(A) tail, we performed the same experiments using luciferase mRNAs lacking poly(A) tails (Fig. S2*B*). In the absence of the poly(A) tail, the PTC readthrough was higher (4%; Fig. S2*C*) than in the presence of the poly(A) tail (2.5%; Fig. 1*C*). The addition of PABP and PAIPs did not alter the PTC readthrough of this mRNA variant (Fig. S2*B*). It suggests that the poly(A) tail is required for PABP and PAIP activities in relation to the PTC. The results obtained in the cell-free translation system indicated that PAIP1 and PAIP2 increased the readthrough of the PTC by controlling PABP activity during translation termination.

PAIP2 prevents binding of PABP and eRF3a in the pulldown assay

To test the effect of PAIP1 and PAIP2 on the interaction of PABP with eRF3a, we performed pulldown assays using PABP bound to magnetic beads and GST-fused PAIP1 and PAIP2. GST-fused PAIP1 and PAIP2 bound to PABP (Fig. 1*D*), which was previously reported (3, 6), and in the presence of eRF3a, PABP retained the ability to bind both PAIP1 and PAIP2 (Fig. 1*D*). Pulldown assays using magnetic beads bound with PABP demonstrated the interaction of PABP with eRF3a alone and with eRF3a in the presence of PAIP1 (Fig. 1*E*). However, binding of PABP to eRF3a in the presence of PAIP2 was less pronounced (Fig. 1*E*). We concluded that PABP could form a ternary complex with PAIP1 and eRF3a. However, the ternary complex of PABP with PAIP2 and eRF3a was undetectable in the pulldown assay.

PAIP2 inhibits the activity of PABP in peptide release assay

Recently, we have shown that PABP stimulates peptide release and termination complexes (TCs) formation in the presence of eRF1 and eRF3a using purified preTCs, containing radiolabeled peptides (30) To determine whether PAIPs interfere with PABP in peptidyl-tRNA hydrolysis, we tested the efficiency of peptide release via the eRF1–eRF3a complex and in the presence of both PABP and PAIPs (Fig. 2*A*). Both PAIP1 and PAIP2 did not influence peptide release induced by release factors; however, after activation of peptide release by the addition of PABP to the release factors, we observed decreasing of peptide release by PAIP2, whereas PAIP1 did not influence under the same conditions. These results indicated that PAIP2 was a stronger inhibitor of PABP during peptidyl-tRNA hydrolysis than PAIP1.

PAIP1 and PAIP2 suppress PABP stimulation of TC formation

We determined the influence of PAIP1 and PAIP2 on the stimulation activity of PABP during TCs formation (Fig. 2, *B* and *C*) using fluorescent toe-printing assay (38). The fluorescent toe-printing assay allows detection of positions of stable ribosomal complexes on mRNA via synthesis using fluorescently labeled primers targeting cDNA products by reverse transcriptase. During stop codon recognition by eRF1, the ribosome protects additional nucleotides on mRNA, which could be detected in the toe-printing assay as a one- or two-nucleotide shift of the ribosomal complex (17, 30). As a result, TC (before peptidyl-tRNA hydrolysis) and postTC (after peptidyl-tRNA hydrolysis) with the same position on mRNA are formed.

We found that in the presence of eRF1 and eRF3a, the simultaneous addition of PAIP1 and PABP or preassociation of PAIP1 with PABP significantly inhibited the effect of PABP on ribosomal shift (Fig. 2*B*). These findings indicated that PAIP1 prevented the binding of the PABP–eRF3a complex to the preTC, thereby removing PABP from the translation termination reaction. Similarly, PAIP2 bound PABP in solution and suppressed PABP-mediated translation activation in the presence of eRF1 and eRF3a (Fig. 2*C*). Therefore, PAIP1 and PAIP2

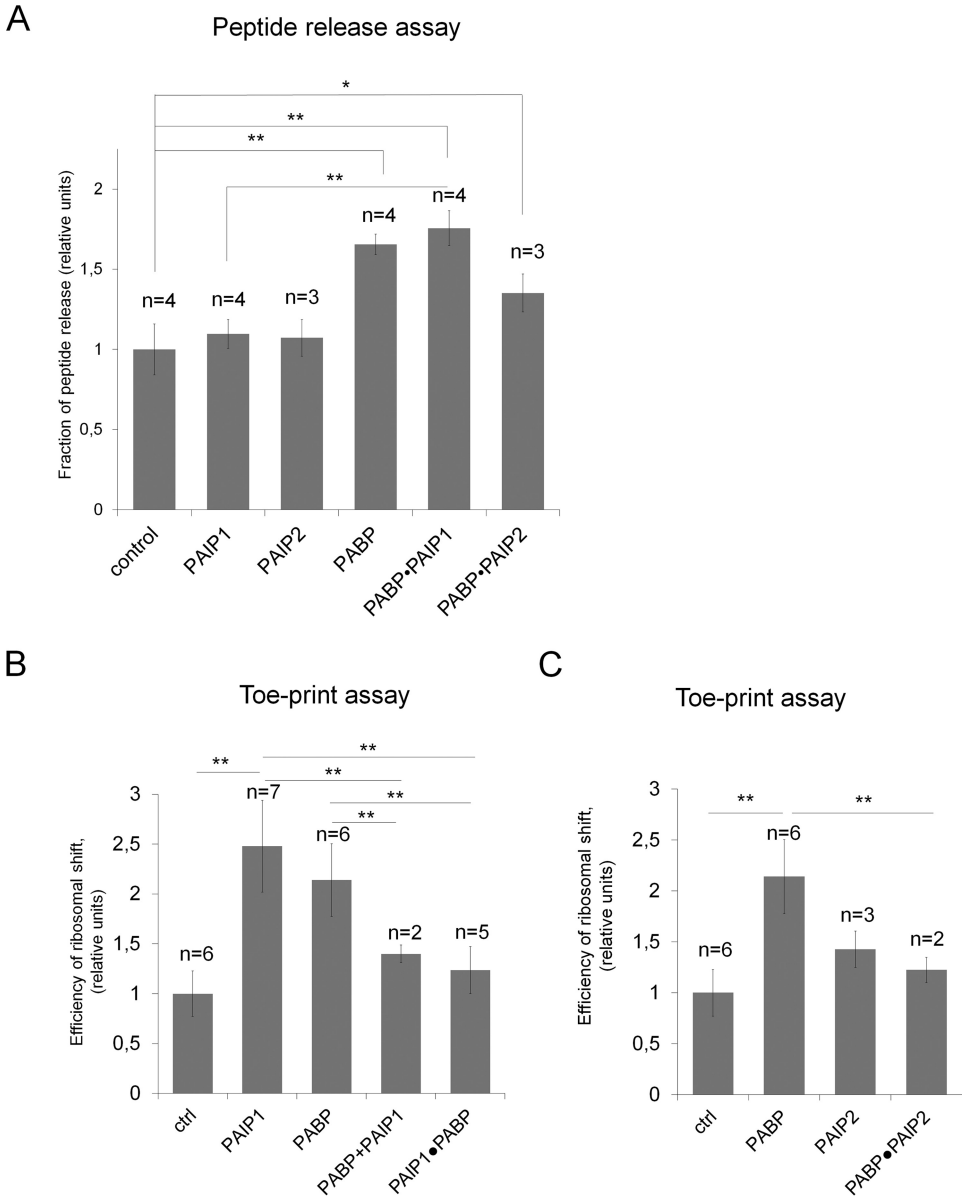

Figure 2. Effect of PAIP1 and PAIP2 on transactivation of translation termination by PABP. *A*, effect of PAIP1 and PAIP2 on PABP-mediated peptide release in the presence of eRF1 and eRF3a. PAIP, PABP, and release factors were preliminarily associated. *B*, effect of PAIP1 and PABP on TC formation in the presence of eRF1 and eRF3a. *C*, effect of PAIP2 and PABP on TC formation in the presence of eRF1 and eRF3a. The background was subtracted, and each mean value was normalized to the value of eRF1 or eRF1 + eRF3 activity, respectively. **, $p < 0.01$; *, $p < 0.05$, *t* test. *n*, number of repeats.

can compete with eRF3a in solution for PABP binding during TC formation.

We previously showed in-*cis* activation of translation termination by PABP bound to the poly(A) tail of mRNA (30). In the present study, to examine the effect of PAIPs on the activity of PABP bound to the poly(A) tail during translation termination, we performed a toe-printing assay of the complexes assembled on MVHC-poly(A) mRNA bound with PABP. First, PABP incubated with poly(A) mRNA, and then ribosomal complexes were assembled from individual components and purified by sucrose gradient centrifugation (Fig. S3*A*).

In translation termination, we compared activities of eRF1–eRF3a and eRF1–eRF3c complexes. eRF3c does not interact with PABP, which excludes the effect of poly(A)-bound PABP on translation termination with this protein. As expected, poly(A)-bound PABP increased TC formation in the presence of eRF3a and did not influence in the presence of eRF3c (Fig. S3*B*). However, the addition of 1 pmol of PAIP1 or PAIP2 was unable to suppress mRNA-bound PABP activity during translation termination (Fig. S3*B*). Additionally, the ability of PAIP1 to stimulate postTC formation in the presence of eRF3a/c was very weak or undetectable under such conditions (Fig. S3*B*). However, higher amounts (4 pmol) of PAIP1/2 in the reaction induced unspecific dissociation of the ribosomal complexes. These results point out the possible influence of binding of PABP to a poly(A) tail on the suppression of its activity by PAIPs.

PAIP1 promotes the postTC formation

Surprisingly, during competition experiments, we observed that PAIP1 alone activated TC/postTC formation in the pres-

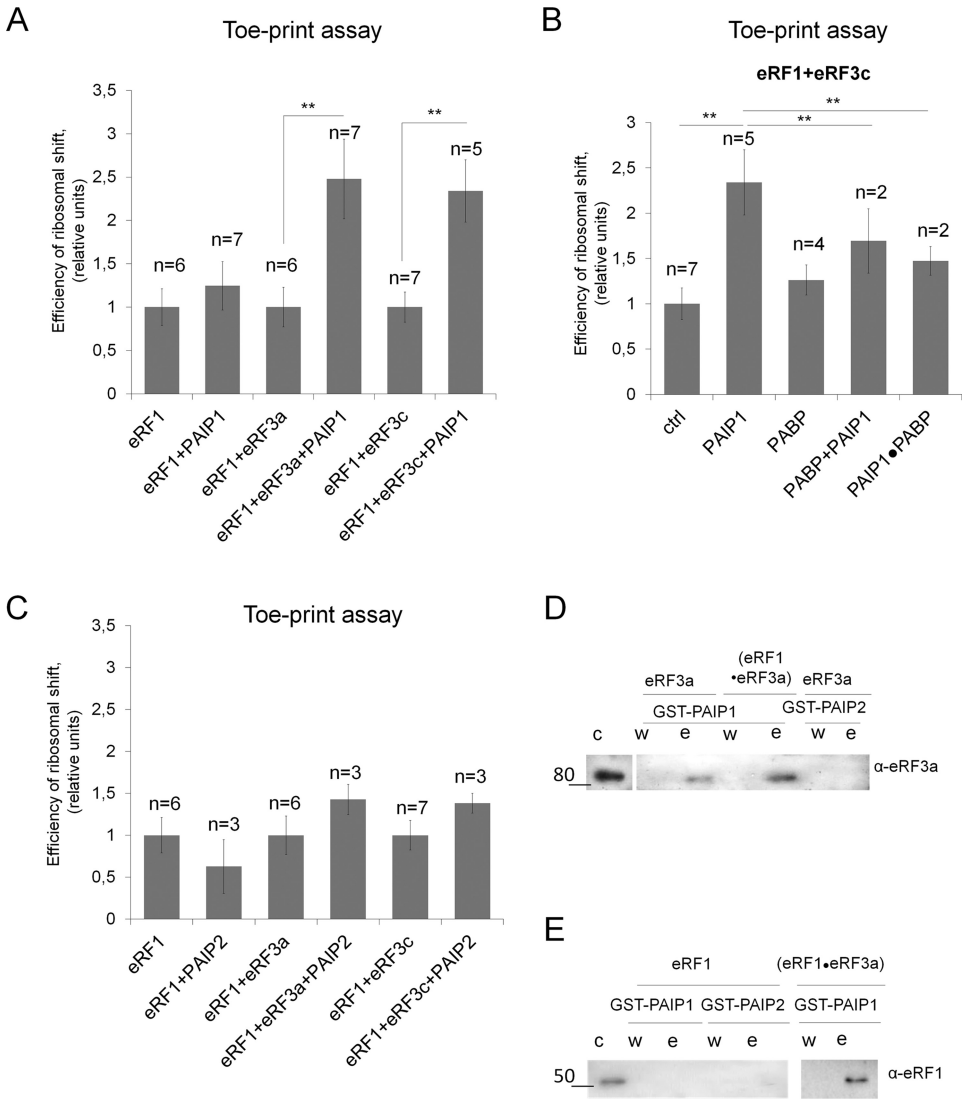

Figure 3. Effect of PAIP1 and PAIP2 on release factors activity. *A*, effect of PAIP1 on TC/postTC formation in the presence of eRF1 and eRF3a/c. *B*, effect of PABP on activation of TC/postTC formation by PAIP1 in the presence of eRF1 and eRF3c. *C*, effect of PAIP2 on TC/postTC formation in the presence of eRF1 and eRF3a/c. The background was subtracted, and each mean value was normalized to the value of eRF1 or eRF1 + eRF3 activity, respectively. **, $p < 0.01$, *t* test. *n*, number of repeats. *D* and *E*, interaction of PAIP1 and PAIP2 with release factors according to GST pulldown assay. PAIP1 and PAIP2 bound with eRF3a or the eRF1–eRF3a complex (*D*) and eRF1 or the eRF1–eRF3a complex (*E*). For detection, antibodies raised against eRF1 and eRF3 were used. *c*, control protein; *w*, wash; *e*, elution by protease cleavage of GST-tagged proteins.

ence of eRF1 and eRF3a and the absence of PABP (Fig. 2*B*). However, PAIP1 was unable to stimulate peptide release (Fig. 2*A*). We proposed that PAIP1 increases the amount of postTC, formed after peptide release. To confirm this hypothesis, we evaluated the activity of PAIP1 and PAIP2 in postTC formation in the absence of PABP. We used two eRF3 variants: the full-length eRF3a and its truncated form lacking 138 N-terminal amino acid residues eRF3c, unable to bind PABP. We found that PAIP1 stimulated postTC formation in the presence of eRF1 and both eRF3 variant (Fig. 3*A*). Notably, PAIP1 did not influence postTC formation in the presence of eRF1 alone (Fig. 3*A*). Because PAIP1 is active during postTC formation in the presence of full-length and truncated eRF3, the mechanism of stimulation likely differs from that of PABP. It is likely that the PAIP1-interacting site of eRF3 is not located in the N-terminal region of the latter. Interestingly, in the presence of a nonhydrolyzable analog of GTP (GDPCP), PAIP1 was unable to stimulate ribosomal shift during translation termination in contrast to PABP (Fig. S4). These findings confirm that PAIP1 is involved in the formation/stabilization of the postTC, which is formed as a result of peptidyl-tRNA hydrolysis, and before dissociation of eRF1 from the ribosome.

We then used eRF3c, which is unable to bind PABP, to detect the effect of PABP on PAIP1 during translation termination. Our results showed that PABP also inhibited PAIP1 activity during postTC formation, likely by removing PAIP1 from the reaction (Fig. 3*B*). These results suggested mutual competition between PAIP1 and PABP during translation termination; however, they did not affect their respective binding activity with eRF3 *in vitro* (Fig. 1, *D* and *E*).

PAIP2 demonstrated only a modest effect on translation termination in the presence of eRF1 and both eRF3 variants (Fig. 3*C*). Considering that PAIP2 lacks a MIF4G domain, which differentiates it from PAIP1 (Fig. 1*A*), our results indicate that

the MIF4G domain is responsible for postTC stabilization by PAIP1.

PAIP1 interacts with eRF3

Because PAIP1 increased postTC formation only in the presence of eRF3a/c, we tested their ability to interact with each other in solution by GST-pulldown assay. We revealed that PAIP1 could bind to eRF3a alone, as well as to eRF3a in the complex with eRF1 (Fig. 3*D*). Moreover, in the experiment in which PAIP1 interaction with the complex eRF1–eRF3a was investigated, we detected binding in a solution of both eRF3a and eRF1 to PAIP1 (Fig. 3*E*). Given that, we did not observe PAIP1 interaction with eRF1 alone (Fig. 3*E*), we speculated that during pulldown assay, PAIP1 interacted with eRF1 via eRF3 to form a ternary complex. As expected, PAIP2 was unable to bind release factors in similar experiments (Fig. 3, *D* and *E*). Therefore, pulldown experiments indicated that PAIP1 could interact with eRF3 in solution and further support the hypothesized involvement of PAIP1 in postTC formation, as previously supposed from the toe-printing assay (Fig. 3*A*).

Discussion

In this study, we revealed the roles of PAIP1 and PAIP2 in translation termination by investigating their influence on PABP, which loads release factors onto the ribosome, and their effect on eRF1 and eRF3. PAIP1 has been described as a translation activator; however, its influence has only been considered in the context of translation initiation (3, 4). Here, we demonstrated a dual and controversial effect of this protein on translation termination. First, PAIP1 suppressed PABP activity in termination during cell-free translation, peptide release, and TC formation (Figs. 1*C* and 2, *A* and *B*). Second, we observed that PAIP1 was able to interact with eRF3 and the eRF3–eRF1 complex in solution and stimulated postTC formation (Fig. 3 and Fig. S4). Although the precise interaction sites remain unclear, we speculated that the MIF4G domain of PAIP1 might be involved in eRF3 binding, given that PAIP1 differs from PAIP2 primarily by the presence of a MIF4G domain, and PAIP2 demonstrated no or very modest effect on release-factor activity (Figs. 2*A* and 3*C*). Because the effect of PAIP1 on translation termination was only observed in the toe-printing assay, we propose that PAIP1 stabilizes the postTC on the ribosome. This mechanism was confirmed by the absence of a shift of ribosomal complex in the presence of PAIP1 and GDPCP (Fig. S4*A*). This suggested that fixation of the closed conformation of eRF3 on the ribosome via a nonhydrolyzable GTP analog eliminated the stimulating effect of PAIP1. On the contrary, PABP remained active in translation termination in the presence of GDPCP, indicating a different mechanism of action of these two proteins (Fig. S4*B*).

It was shown earlier that PAIP2 decreases translation efficiency; however, most studies focus on its involvement in translation initiation (6). In the present study, we found that interaction of PAIP2 with free PABP suppressed PABP activity during translation termination even stronger than we observed for PAIP1 both *in vitro* according to a peptide release assay (Fig. 2*A*) and during cell-free translation (Fig. 1*C*). Strong inhibition of translation termination by PAIP2 can be explained by its PABP binding activity, which is stronger than that of eRF3a (Fig. 1*E*). The weaker effect of PAIP1 on termination can be explained by PABP-PAIP1-eRF3a ternary complex formation (Fig. 1, *D* and *E*). We propose that such a complex forms as a result of simultaneous interaction of different parts of PAIP1 with PABP and eRF3a. After displacement of eRF3a from the PABP–eRF3a complex, PAIP1 can bind to PABP via PAM1 and PAM2 domains and to eRF3a via MIF4G domain (Fig. 1, *A*, *D*, and *E*).

By contrast to the trans-activity of PABP in termination, both PAIP1 and PAIP2 did not inhibit the termination activity of PABP bound to the poly(A) tail of mRNA (Fig. S3*B*). The absence of a PAIP2-specific effect on poly(A)-bound PABP during translation termination is consistent with a previous report, demonstrating that PAIP2 cannot interact with poly(A)-bound PABP (15). We proposed that PAIP1 and PAIP2 are unable to influence PABP during translation termination when the latter is bound to mRNA. However, our findings revealed that in a cell lysate, PAIPs suppress translation termination of only poly(A)-containing mRNAs (Fig. 1*C* and Fig. S3*B*). These results suggested that in the cell, the poly(A) tail on mRNA accumulates PABP molecules in the immediate vicinity, thereby increasing its local concentration in solution as a result of reaching dynamic equilibrium. These PABP molecules might be involved in binding to the eRF1–eRF3 complex in solution and subsequent stimulation of translation termination at PTCs and production of nonfunctional truncated peptides.

In summary, our data highlighted the roles of PAIP1 and PAIP2 in translation termination and advanced the current view on translational control in higher eukaryotes. Based on our findings, we propose a model of PABP regulation during translation termination (Fig. 4). To prevent premature termination, PAIP1 and PAIP2 bind the solution fraction of PABP via both PAM1 and PAM2 motifs, which excludes it from interacting with release-factor complexes (Fig. 4, *B* and *C*). Termination at the PTC consequently becomes inefficient and can be suppressed by readthrough via the activity of a suppressor, near-cognate tRNAs, or induction of the nonsense-mediated decay mechanism. By contrast, termination at native stop codons is unaffected by PAIPs because of the proximity of poly(A) tails bound with PABP via the closed-loop mRNA structure. Additionally, poly(A)-bound PABP might allow localization of eRF3 or the eRF3–eRF1 complex in the proximity of mRNA to ensure rapid translation termination (Fig. 4, *A* and *C*). Similarly, the binding of PAIP1 with eRF3 via the MIF4G domain might also address the same problem (Fig. 4*B*).

We observed that the addition of PAIPs to cell lysate increased PTC readthrough 2-fold, which was ~4% of all the translation termination events (Fig. 1*C*). It means that 96% of the synthesized protein at PTC-containing mRNA would be truncated and inactive. However, even an additional small percentage of PTC readthrough is vital for cells. Several genetic diseases lose their lethality because of increased PTC readthrough, and even 4% to 5% of the production of full-length proteins can support the existence of an organism and offer an evolutionary advantage. The main factor that determines the efficiency of PTC readthrough concerns the minimum level of deficient protein function that needs to be restored to achieve a

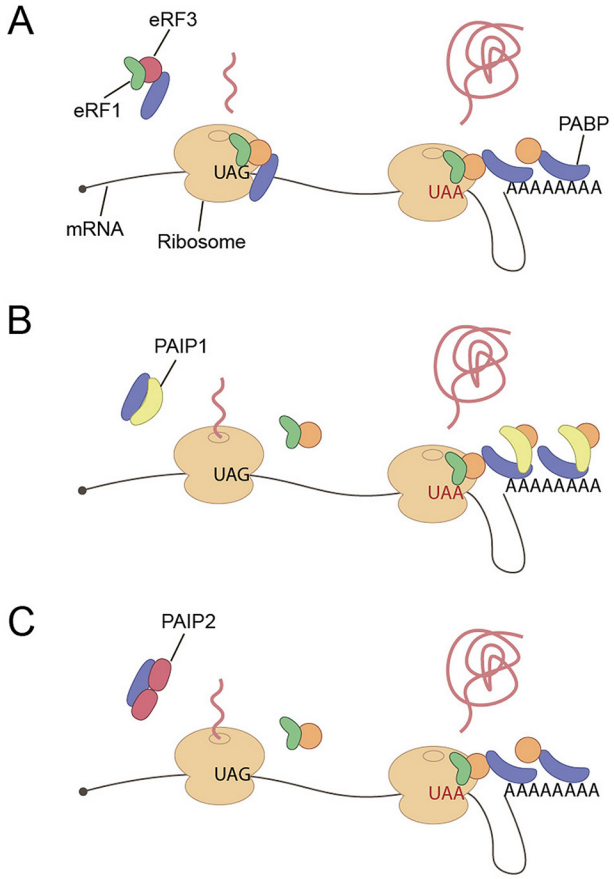

Figure 4. Model of the effect of PAIP1 and PAIP2 on translation termination. *A*, stimulation of premature translation termination by the non–poly(A)-bound form of PABP. *B* and *C*, PAIP1- and PAIP2-mediated suppression of translation termination by the unbound form of PABP.

therapeutic improvement. This varies significantly for different diseases. For example, 30–35% of normal cystic fibrosis transmembrane conductance regulator activity is required for a therapeutic improvement in cystic fibrosis, 20–30% of normal dystrophin function is required for attenuation of Duchenne muscular dystrophy, and 0.4–1% of α-L-iduronidase enzyme activity is required to alleviate mucopolysaccharidosis type I (Hurler syndrome) (39).

Experimental procedures

PAIP1 and PAIP2 cloning and purification

Human PAIP1 cDNA (corresponding to isoform 1 mRNA) and PAIP2 cDNA were cloned into the pGEX-6p-1 vector (GE Healthcare) between BamHI/XhoI sites. The resulting GST-tagged proteins were expressed in *Escherichia coli* Rosetta cells (Novagen, Madison, WI) after induction by 1 mM isopropyl β-D-thiogalactopyranoside at 25 °C overnight, followed by purification using a GSH-Sepharose column (GE Healthcare) and elution by either PreScission protease (GE Healthcare), which cleaves a GST tag from the protein, or 5 mM GSH in buffer comprising 50 mM Tris HCl (pH 7.0), 100 mM KCl, 10 mM DTT, and 5% glycerol. Eluted proteins with or without GST tag were then applied to a HiTrapQ column (GE Healthcare) and purified by KCl gradient 100–500 mM.

mRNA transcription for luciferase assay

The pGEM-luc plasmid (Promega, Madison, WI) contains a short 5′-UTR (56 nt) and a firefly luciferase gene, followed by a short 3′-UTR (60 nt). The pGEM-luc-STOP plasmid contains the same gene with a PTC UGA instead of Ser-447 and encodes a nonfunctional C-terminally truncated firefly luciferase gene unless this PTC is readthrough. The transcription template was obtained by PCR using a forward primer bearing the T7 promoter sequence and a reverse primer complementary to the 3′-UTR, which either contained 50 thymine residues or did not. PCR fragments were purified by agarose gel electrophoresis, and transcription with T7 polymerase was performed according to manufacturer protocol (Promega). mRNAs were purified by precipitation in 2.5 M LiCl and capped using the Vaccinia capping system (New England Biolabs).

Luciferase assay

The translation was performed in nuclease untreated Krebs-2-ascites cytoplasmic extract, as previously described (35). Translation mixture contained 20 mM HEPES-KOH (pH 7.0), 120 mM KOAc, 1.2 mM $Mg(OAc)_2$, 2 mM DTT, 0.5 mM spermidine, 1 mM ATP, 0.2 mM GTP, 0.03 mM of each amino acid, 0.2 unit/μl RNase inhibitor, 0.5 mM D-luciferin (Promega), 8 mM creatine phosphate, and 50% nuclease-untreated Krebs-2 lysate (S30). Reporter mRNA (0.15 pmol) and different amounts of tested proteins (1.5 pmol of PABPC1, 2 pmol of PAIP1, or 0.5 pmol of PAIP2) were added to 10 μl of translation mixture, and luminescence was measured at 30 °C using a Tecan Infinite 200Pro (Tecan, Männedorf, Switzerland). The translation rate was calculated as a derivative of the first linear section of the luminescence curve (Fig. S1). PTC readthrough was calculated using the formula (translation rate of the PTC-luc mRNA/translation rate of the luc mRNA) × 100%.

GST pulldown assay

GST-PAIP1 or GST-PAIP2 (40 pmol) were incubated with 40 pmol protein of interest in binding buffer containing 25 mM Tris-HCl (pH 7.5), 100 mM KCl, 2.5 mM $MgCl_2$, 2 mM DTT, 0.25 mM spermidine, and 0.2 mM GTP equilibrated with $MgCl_2$ at a final volume of 20 μl. The reaction mixture was incubated for 10 min at 37 °C, followed by the addition of 20 μl of 50% GSH-Sepharose (equilibrated with the same buffer) and incubation for 5 min at 37 °C with shaking. After centrifugation, the supernatant was removed, and the resin was washed three times with 500 μl and once with 20 μl of binding buffer without nucleotides. Following the final wash, 15 μl of supernatant was used for Western blotting analysis as a negative control. 1 μl of PreScission protease (GE Healthcare) diluted in 15 μl of binding buffer was added to the resin for 10 min at 37 °C, after which 15 μl of supernatant was used for Western blotting analysis with corresponding antibodies.

Magnetic bead pulldown assay

PAIP1, PAIP2, or eRF3a (30 pmol) were incubated with 30 pmol of PABP cross-linked to magnetic beads (Glyoxal-activated agarose-covered beads) in PBS buffer containing 1.8 mM

KH_2PO_4, 10 mM Na_2HPO_4, 2.7 mM KCl, 137 mM NaCl with 5% milk, 0.1% Triton X-100, 2.5 mM $MgCl_2$, 2 mM DTT, 0.2 mM GTP equilibrated with $MgCl_2$, RNase A 5u at a final volume of 50 μl. The reaction mixture was incubated for 10 min at 37 °C with gentle shaking. Using the magnetic rack, the beads were collected, the supernatant was removed, and the beads were washed three times with 500 μl of PBS + 0.5% Triton X-100. The fourth wash was performed overnight. Following the final wash, 10 μl of supernatant were used for Western blotting analysis as a negative control. The beads with interacting proteins were resuspended in 10 μl of gel loading buffer and used for Western blotting analysis with corresponding antibodies.

Pretermination complex assembly

The 40S and 60S ribosomal subunits, as well as eukaryotic translation factors eIF2, eIF3, eEF1H, and eEF2, were purified from a rabbit reticulocyte lysate, as previously described (17). The human translation factors eIF1, eIF1A, eIF4A, eIF4B, ΔeIF4G, ΔeIF5B, eIF5, PABP, and eRF1 were produced as recombinant proteins in *E. coli* strain BL21 with subsequent protein purification on nickel–nitrilotriacetic acid–agarose and ion-exchange chromatography (17). Human eRF3a was expressed in insect cells Sf21 and purified by affinity chromatography using a HisTrap HP column (GE Healthcare) followed by anion-exchange chromatography using a MonoQ column (GE Healthcare) (30).

mRNAs were transcribed by T7 RNA polymerase from pET28-MVHL-UAA, pUC57-MVHC-poly(A) plasmids. pET28-MVHL-UAA plasmid contains T7 promoter, four CAA repeats, the β-globin 5′-UTR, ORF (encoding for the peptide MVHL), followed by the stop codon UAA and a 3′-UTR comprising the rest of the natural β-globin coding sequence. For run-off, transcription mRNA plasmids were linearized with XhoI. The pUC57-MVHC-poly(A) plasmid contains T7 promoter, four CAA repeats, the β-globin 5′-UTR, ORF (encoding the peptide MVHC) followed by the stop codon UAA, the β-globin 3′-UTR, and 50 adenine residues. For run-off, transcription mRNA plasmids were linearized with EcoRI (30).

Either ^{35}S-labeled or unlabeled eukaryotic preTC on MVHL-UAA mRNA were assembled and purified as previously described (37). Briefly, initiation complexes were assembled in a 500-μl solution containing 37 pmol of MVHL-lessC mRNA or MVHL-stop mRNA, 200 pmol of Met-tRNAiMet, or ^{35}S-labeled Met-tRNAiMet, 90 pmol of 40S and 60S ribosomal subunits, 200 pmol of eIF2, 90 pmol of eIF3, and 125 pmol of eIF4A, ΔeIF4G (p50), eIF4B, eIF1, eIF1A, eIF5, and ΔeIF5B, respectively, supplemented with buffer A (25 mM Tris-HCl, pH 7.5, 50 mM KOAc, 2.5 mM $MgCl_2$, 2 mM DTT, 0.3 unit/μl RNase inhibitor, 1 mM ATP, 0.25 mM spermidine, and 0.2 mM GTP). The reaction mixture was maintained at 37 °C for 15 min to allow ribosomal–mRNA complex formation. Peptide elongation was performed by the addition of 200 pmol of total tRNA (acylated with all or individual amino acids), 200 pmol of eEF1H, and 50 pmol of eEF2 to the initiation complex, followed by incubation for another 15 min at 37 °C. The ribosomal complexes were centrifuged in a Beckman SW55 rotor for 95 min at 4 °C and 50,000 rpm in a linear sucrose density gradient (10–30%, w/w) prepared in buffer A containing 5 mM $MgCl_2$. Fractions corresponding to preTC complexes were detected by toe-printing assay and by the presence of [^{35}S]Met. The preTC fractions were combined and diluted 3-fold with buffer A containing 1.25 mM $MgCl_2$ (to a final concentration of 2.5 mM Mg^{2+}) and used in the peptide-release assay or for conformation-rearrangement analysis. PreTC on MVHC-poly(A) was assembled in the presence of 160 pmol of PABPC1 and purified as previously described (30).

Peptide release assay

Radiolabeled preTCs (0.1 pmol), assembled on MVHL-UAA mRNA, were incubated in 30 μl of the reaction mixture with 0.2 pmol of eRF3a and 0.2 pmol of eRF1, and 4 pmol of either PAIP1 or PAIP2, at 37 °C for 3 min. In the competition experiments, complexes eRF1–eRF3a–protein of interest (containing 0.2 pmol of eRF3a and 0.2 pmol of eRF1, and 4 pmol of PAIP1, PAIP2, PABPC1, or their combination) were preassembled at 37 °C for 1 min, followed by their addition to preTC along with 0.2 mM GTP and 0.2 mM $MgCl_2$ and incubation at 37 °C for 3 min. Ribosomes and tRNA were pelleted with ice-cold 5% TCA and centrifuged at 14,000 × *g* at 4 °C. The amount of released ^{35}S-containing peptide was determined by scintillation counting of supernatants using an Intertechnique SL-30 liquid scintillation spectrometer (37).

Toe-printing assay

We dissolved 0.03 pmol of preTCs in 10 μl of reaction mixture, assembled on MVHL-stop mRNA, and incubated with 0.6 pmol of eRF1 or eRF1(AGQ) mutant, 0.6 pmol of eRF3a or eRF3c, and 4 pmol of proteins of interest or their combinations (PAIP1, PAIP2, or PABPC1) at 37 °C for 10 min in the presence of 0.2 mM GTP and supplemented with equimolar amounts of $MgCl_2$. In addition, 0.03 pmol of preTCs were added to 10 μl of reaction mixture, assembled on MVHC-poly(A) mRNA in the presence of PABP and incubated with 0.6 pmol of eRF1(AGQ) mutant, 0.6 pmol of eRF3a or eRF3c, and 1 pmol of PAIP1 or PAIP2 at 37 °C for 10 min in the presence of 0.2 mM GTP and supplemented with equimolar amounts of $MgCl_2$.

The samples were analyzed using a primer extension protocol. The toe-printing analysis was performed with avian myeloblastosis virus reverse transcriptase and 5′-6-carboxyfluorescein-labeled primers complementary to 3′-UTR sequences. cDNAs were separated by electrophoresis using standard GeneScan® conditions on an ABI Prism® Genetic Analyzer 3100 (Applera).

Conformational rearrangements corresponding to TC or postTC formation were detected as a +2-nt shift at MVHL-UAA mRNA) or a +1-nt shift at MVHC-poly(A) mRNA of toe-print peaks, as previously described (30, 36–38). Ribosomal shift efficiency was calculated using the formula TC/(TC+ preTC). All data were normalized according to the ribosomal shift efficiency calculated in control experiments.

Author contributions—A. I., I. T., and E. A. conceptualization; A. I., E. Shuvalova, T. E., A. S., E. Sokolova, N. B., and E. A. investigation; A. I. methodology; A. I., I. T., and E. A. writing-original draft; I. S., I. T., and E. A. writing-review and editing; I. T. and E. A. supervision; E. A. funding acquisition.

Acknowledgments—We are grateful to Ludmila Frolova for providing us with plasmids encoding release factors; to Tatyana Pestova and Christopher Hellen, who provided us with plasmids encoding initiation factors; and to Christiane Schaffitzel, who provided us with plasmids encoding eRF3a, PABP, and MVHC-poly(A) mRNA. cDNA-fragment analyses were performed by the center of the collective use "Genome" of the Engelhardt Institute of Molecular Biology of the Russian Academy of Sciences.

References

1. Deo, R. C., Bonanno, J. B., Sonenberg, N., and Burley, S. K. (1999) Recognition of polyadenylate RNA by the poly(A)-binding protein. *Cell* **98,** 835–845 CrossRef Medline
2. Kozlov, G., and Gehring, K. (2010) Molecular basis of eRF3 recognition by the MLLE domain of poly(A)-binding protein. *PLoS One* **5,** e10169 CrossRef Medline
3. Craig, A. W., Haghighat, A., Yu, A. T., and Sonenberg, N. (1998) Interaction of polyadenylate-binding protein with the eIF4G homologue PAIP enhances translation. *Nature* **392,** 520–523 CrossRef Medline
4. Roy, G., De Crescenzo, G., Khaleghpour, K., Kahvejian, A., O'Connor-McCourt, M., and Sonenberg, N. (2002) Paip1 interacts with poly(A) binding protein through two independent binding motifs. *Mol. Cell. Biol.* **22,** 3769–3782 CrossRef Medline
5. Khaleghpour, K., Kahvejian, A., De Crescenzo, G., Roy, G., Svitkin, Y. V., Imataka, H., O'Connor-McCourt, M., and Sonenberg, N. (2001) Dual interactions of the translational repressor Paip2 with poly(A) binding protein. *Mol. Cell. Biol.* **21,** 5200–5213 CrossRef Medline
6. Khaleghpour, K., Svitkin, Y. V., Craig, A. W., DeMaria, C. T., Deo, R. C., Burley, S. K., and Sonenberg, N. (2001) Translational repression by a novel partner of human poly(A) binding protein, Paip2. *Mol. Cell* **7,** 205–216 CrossRef Medline
7. Eliseeva, I. A., Lyabin, D. N., and Ovchinnikov, L. P. (2013) Poly(A)-binding proteins: structure, domain organization, and activity regulation. *Biochemistry* (*Mosc.*) **78,** 1377–1391 CrossRef Medline
8. Imataka, H., Gradi, A., and Sonenberg, N. (1998) A newly identified N-terminal amino acid sequence of human eIF4G binds poly(A)-binding protein and functions in poly(A)-dependent translation. *EMBO J.* **17,** 7480–7489 CrossRef Medline
9. Kahvejian, A., Svitkin, Y. V., Sukarieh, R., M'Boutchou, M. N., and Sonenberg, N. (2005) Mammalian poly(A)-binding protein is a eukaryotic translation initiation factor, which acts via multiple mechanisms. *Genes Dev.* **19,** 104–113 CrossRef Medline
10. Borman, A. M., Michel, Y. M., and Kean, K. M. (2000) Biochemical characterisation of cap-poly(A) synergy in rabbit reticulocyte lysates: the eIF4G-PABP interaction increases the functional affinity of eIF4E for the capped mRNA 5′-end. *Nucleic Acids Res.* **28,** 4068–4075 CrossRef Medline
11. Wells, S. E., Hillner, P. E., Vale, R. D., and Sachs, A. B. (1998) Circularization of mRNA by eukaryotic translation initiation factors. *Mol. Cell* **2,** 135–140 CrossRef Medline
12. Rajkowitsch, L., Vilela, C., Berthelot, K., Ramirez, C. V., and McCarthy, J. E. (2004) Reinitiation and recycling are distinct processes occurring downstream of translation termination in yeast. *J. Mol. Biol.* **335,** 71–85 CrossRef Medline
13. Costello, J., Castelli, L. M., Rowe, W., Kershaw, C. J., Talavera, D., Mohammad-Qureshi, S. S., Sims, P. F., Grant, C. M., Pavitt, G. D., Hubbard, S. J., and Ashe, M. P. (2015) Global mRNA selection mechanisms for translation initiation. *Genome Biol.* **16,** 10 Medline
14. Martineau, Y., Derry, M. C., Wang, X., Yanagiya, A., Berlanga, J. J., Shyu, A. B., Imataka, H., Gehring, K., and Sonenberg, N. (2008) Poly(A)-binding protein-interacting protein 1 binds to eukaryotic translation initiation factor 3 to stimulate translation. *Mol. Cell. Biol.* **28,** 6658–6667 CrossRef Medline
15. Lee, S. H., Oh, J., Park, J., Paek, K. Y., Rho, S., Jang, S. K., and Lee, J. B. (2014) Poly(A) RNA and Paip2 act as allosteric regulators of poly(A)-binding protein. *Nucleic Acids Res.* **42,** 2697–2707 CrossRef Medline
16. Karim, M. M., Svitkin, Y. V., Kahvejian, A., De Crescenzo, G., Costa-Mattioli, M., and Sonenberg, N. (2006) A mechanism of translational repression by competition of Paip2 with eIF4G for poly(A) binding protein (PABP) binding. *Proc. Natl. Acad. Sci. U.S.A.* **103,** 9494–9499 CrossRef Medline
17. Alkalaeva, E. Z., Pisarev, A. V., Frolova, L. Y., Kisselev, L. L., and Pestova, T. V. (2006) In vitro reconstitution of eukaryotic translation reveals cooperativity between release factors eRF1 and eRF3. *Cell* **125,** 1125–1136 CrossRef Medline
18. Zhouravleva, G., Frolova, L., Le Goff, X., Le Guellec, R., Inge-Vechtomov, S., Kisselev, L., and Philippe, M. (1995) Termination of translation in eukaryotes is governed by two interacting polypeptide chain release factors, eRF1 and eRF3. *EMBO J.* **14,** 4065–4072 CrossRef Medline
19. Feng, T., Yamamoto, A., Wilkins, S. E., Sokolova, E., Yates, L. A., Münzel, M., Singh, P., Hopkinson, R. J., Fischer, R., Cockman, M. E., Shelley, J., Trudgian, D. C., Schödel, J., McCullagh, J. S., Ge, W., *et al.* (2014) Optimal translational termination requires C4 lysyl hydroxylation of eRF1. *Mol. Cell* **53,** 645–654 CrossRef Medline
20. Song, H., Mugnier, P., Das, A. K., Webb, H. M., Evans, D. R., Tuite, M. F., Hemmings, B. A., and Barford, D. (2000) The crystal structure of human eukaryotic release factor eRF1: mechanism of stop codon recognition and peptidyl-tRNA hydrolysis. *Cell* **100,** 311–321 CrossRef Medline
21. Eliseev, B., Kryuchkova, P., Alkalaeva, E., and Frolova, L. (2011) A single amino acid change of translation termination factor eRF1 switches between bipotent and omnipotent stop-codon specificity. *Nucleic Acids Res.* **39,** 599–608 CrossRef Medline
22. Kryuchkova, P., Grishin, A., Eliseev, B., Karyagina, A., Frolova, L., and Alkalaeva, E. (2013) Two-step model of stop codon recognition by eukaryotic release factor eRF1. *Nucleic Acids Res.* **41,** 4573–4586 CrossRef Medline
23. Alkalaeva, E., and Mikhailova, T. (2017) Reassigning stop codons via translation termination: how a few eukaryotes broke the dogma. *Bioessays* **39,** 201600213 CrossRef Medline
24. Dubovaia, V. I., Kolosov, P. M., Alkalaeva, E. Z., Frolova, L., and Kiselev, L. L. (2006) Influence of individual domains of the translation termination factor eRF1 on induction of the GTPase activity of the translation termination factor eRF3. *Mol. Biol.* (*Mosk.*) **40,** 310–316 Medline
25. Brown, A., Shao, S., Murray, J., Hegde, R. S., and Ramakrishnan, V. (2015) Structural basis for stop codon recognition in eukaryotes. *Nature* **524,** 493–496 CrossRef Medline
26. des Georges, A., Hashem, Y., Unbehaun, A., Grassucci, R. A., Taylor, D., Hellen, C. U., Pestova, T. V., and Frank, J. (2014) Structure of the mammalian ribosomal pre-termination complex associated with eRF1.eRF3.GDPNP. *Nucleic Acids Res.* **42,** 3409–3418 CrossRef Medline
27. Preis, A., Heuer, A., Barrio-Garcia, C., Hauser, A., Eyler, D. E., Berninghausen, O., Green, R., Becker, T., and Beckmann, R. (2014) Cryoelectron microscopic structures of eukaryotic translation termination complexes containing eRF1-eRF3 or eRF1-ABCE1. *Cell Rep.* **8,** 59–65 CrossRef Medline
28. Kong, C., Ito, K., Walsh, M. A., Wada, M., Liu, Y., Kumar, S., Barford, D., Nakamura, Y., and Song, H. (2004) Crystal structure and functional analysis of the eukaryotic class II release factor eRF3 from *S. pombe*. *Mol. Cell* **14,** 233–245 Medline
29. Hoshino, S., Imai, M., Kobayashi, T., Uchida, N., and Katada, T. (1999) The eukaryotic polypeptide chain releasing factor (eRF3/GSPT) carrying the translation termination signal to the 3′-poly(A) tail of mRNA. Direct association of erf3/GSPT with polyadenylate-binding protein. *J. Biol. Chem.* **274,** 16677–16680 CrossRef Medline
30. Ivanov, A., Mikhailova, T., Eliseev, B., Yeramala, L., Sokolova, E., Susorov, D., Shuvalov, A., Schaffitzel, C., and Alkalaeva, E. (2016) PABP enhances release factor recruitment and stop codon recognition during translation termination. *Nucleic Acids Res.* **44,** 7766–7776 CrossRef Medline
31. Ivanov, P. V., Gehring, N. H., Kunz, J. B., Hentze, M. W., and Kulozik, A. E. (2008) Interactions between UPF1, eRFs, PABP and the exon junction complex suggest an integrated model for mammalian NMD pathways. *EMBO J.* **27,** 736–747 CrossRef Medline

32. Swart, E. C., Serra, V., Petroni, G., and Nowacki, M. (2016) Genetic codes with no dedicated stop codon: context-dependent translation termination. *Cell* **166,** 691–702 CrossRef Medline
33. Heaphy, S. M., Mariotti, M., Gladyshev, V. N., Atkins, J. F., and Baranov, P. V. (2016) Novel ciliate genetic code variants including the reassignment of all three stop codons to sense codons in *Condylostoma magnum*. *Mol. Biol. Evol.* **33,** 2885–2889 CrossRef Medline
34. Záhonová, K., Kostygov, A. Y., Ševčíková, Yurchenko, V., and Eliáš, M. (2016) An unprecedented non-canonical nuclear genetic code with all three termination codons reassigned as sense codons. *Curr. Biol.* **26,** 2364–2369 CrossRef Medline
35. Andreev, D. E., Dmitriev, S. E., Terenin, I. M., Prassolov, V. S., Merrick, W. C., and Shatsky, I. N. (2009) Differential contribution of the m7G-cap to the 5′ end-dependent translation initiation of mammalian mRNAs. *Nucleic Acids Res.* **37,** 6135–6147 CrossRef Medline
36. Susorov, D., Mikhailova, T., Ivanov, A., Sokolova, E., and Alkalaeva, E. (2015) Stabilization of eukaryotic ribosomal termination complexes by deacylated tRNA. *Nucleic Acids Res.* **43,** 3332–3343 CrossRef Medline
37. Mikhailova, T., Shuvalova, E., Ivanov, A., Susorov, D., Shuvalov, A., Kolosov, P. M., and Alkalaeva, E. (2017) RNA helicase DDX19 stabilizes ribosomal elongation and termination complexes. *Nucleic Acids Res.* **45,** 1307–1318 CrossRef Medline
38. Shirokikh, N. E., Alkalaeva, E. Z., Vassilenko, K. S., Afonina, Z. A., Alekhina, O. M., Kisselev, L. L., and Spirin, A. S. (2010) Quantitative analysis of ribosome-mRNA complexes at different translation stages. *Nucleic Acids Res.* **38,** e15 CrossRef Medline
39. Keeling, K. M., Xue, X., Gunn, G., and Bedwell, D. M. (2014) Therapeutics based on stop codon readthrough. *Annu. Rev. Genomics Hum. Genet.* **15,** 371–394 CrossRef Medline